Orbital Nematic Instability in Two-Orbital Hubbard Model: A Renormalization-Group Study

Masahisa Tsuchiizu,[1] Seiichiro Onari,[2] and Hiroshi Kontani[1]

[1]*Department of Physics, Nagoya University, Nagoya 464-8602, Japan*
[2]*Department of Applied Physics, Nagoya University, Nagoya 464-8603, Japan*

(Dated: September 17, 2012)

Motivated by the nematic electronic fluid phase in $Sr_3Ru_2O_7$, we analyze the (d_{xz}, d_{yz})-orbital Hubbard model by the one-loop renormalization-group method. It is confirmed that the present model exhibits the ferro-orbital instability near the magnetic or superconducting quantum criticality, due to the Aslamazov-Larkin type vertex corrections. This mechanism of orbital nematic order presents a natural explanation for the nematic order in $Sr_3Ru_2O_7$, and is expected to be realized in various multiorbital systems, such as Fe-based superconductors.

PACS numbers: 74.70.Pq, 75.25.Dk, 71.27.+a, 71.10.Fd

A bilayer ruthenate compound $Sr_3Ru_2O_7$ has attracted much attention since it exhibits a unique quantum critical behavior [1–4]. Field-induced antiferromagnetic quantum criticality is observed by the many experiments like the NMR measurements [5]. Surprisingly, the magnetic quantum critical point is hidden by the formation of the nematic electronic liquid phase at very low temperatures ($\sim$ 1K). The orientational-symmetry breaking in the nematic phase is confirmed by the large anisotropy of in-plane resistivity [4, 6, 7]. Thus, the quantum criticality and nematic phase formation are intimately linked in this material [4].

The band structure of the ruthenate oxides are composed of the Ru t_{2g} (d_{xy}, d_{xz}, and d_{yz}) orbitals. For the microscopic understanding of the nematic phase in $Sr_3Ru_2O_7$, a large number of theoretical works have been devoted. The spontaneous violation of the C_4 symmetry of the Fermi surface (FS), i.e., Pomeranchuk instability, had been frequently discussed by focusing on the van Hove singularity. The scenario of *the single-band Pomeranchuk instability* was originally proposed by using the renormalization-group (RG) method [8], and have been analyzed by the mean-field [9–12] and perturbation [13] studies. However, the temperature-flow (T-flow) RG scheme [14, 15] indicates that the nematic instability might be hidden by magnetic instabilities. Thus, the possibility of the single-band Pomeranchuk instability is not settled yet.

Alternative theoretical route to elucidate the nematic phase is to focus on the two d_{xz} and d_{yz} orbitals, which give rise to quasi-one-dimensional (Q1D) α and β bands. It has been pointed out that the nematic state is described as an orbital ordering ($\langle n_{xz}\rangle \neq \langle n_{yz}\rangle$). This *ferro-orbital-order* scenario has been analyzed within the mean-field-level approximation by focusing only on the $\boldsymbol{q} = \boldsymbol{0}$ modes [16–18]. However, the random phase approximation (RPA) leads to the occurrence of the antiferro-orbital order because of the nesting of the FS [19]. Therefore, the theoretical analysis beyond the RPA is required.

Recently, similar nematic phase in Fe-based superconductors, which is also a multiorbital system, attracts great attentions [20, 21]. Up to now, both the spin nematic [22] and orbital nematic [23] theories had been proposed. The latter theory pointed out the importance of the vertex correction (VC) in the nematic order. However, they studied a limited number of VCs, so the importance of VCs should be clarified by other unbiased theoretical techniques. For this purpose, the RG treatment is quite suitable because the RG method enable us to perform the systematic calculations of higher-order VCs.

In this paper, we propose a novel mechanism of the nematic electronic state related to the orbital degrees of freedom, by applying the one-loop RG method to the (d_{xz}, d_{yz})-orbital Hubbard model for the first time. We find that the strong orbital nematic fluctuation, i.e., *orbital Pomeranchuk instability*, emerges near the magnetic or superconducting quantum criticality due to the VCs. The present study indicates that the two-orbital single-layer Hubbard model is a minimal model to describe the orbital nematic order realized in $Sr_3Ru_2O_7$.

We consider a single-layer (d_{xz}, d_{yz})-orbital model, where the orbital index $\mu = 1$ and 2 refer to d_{xz} and d_{yz}, respectively. The tight-binding Hamiltonian with tetragonal symmetry is given in the form

$$H_0 = \sum_{\boldsymbol{k},\sigma} \sum_{\mu,\mu'=1,2} \xi_{\boldsymbol{k}}^{\mu\mu'} c_{\boldsymbol{k},\mu,\sigma}^{\dagger} c_{\boldsymbol{k},\mu',\sigma}, \tag{1}$$

where $\xi_{\boldsymbol{k}}^{11} = -2t\cos k_x - \bar{\mu}$, $\xi_{\boldsymbol{k}}^{22} = -2t\cos k_y - \bar{\mu}$, and $\xi_{\boldsymbol{k}}^{12} = \xi_{\boldsymbol{k}}^{21} = 4t' \sin k_x \sin k_y$, with $\bar{\mu}$ being the chemical potential. We put $(t, t') = (1, 0.1)$ which corresponds to Ru-oxides. We describe the electron-electron interaction by

$$\begin{aligned} H_{\rm int} &= U \sum_{j,\mu=1,2} n_{j,\mu,\uparrow} n_{j,\mu,\downarrow} + U' \sum_j n_{j,1} n_{j,2} \\ &+ J \sum_{j,\sigma,\sigma'} c_{j,1,\sigma}^{\dagger} c_{j,2,\sigma} c_{j,2,\sigma'}^{\dagger} c_{j,1,\sigma'} \\ &+ J \sum_j (c_{j,1,\uparrow}^{\dagger} c_{j,2,\uparrow} c_{j,1,\downarrow}^{\dagger} c_{j,2,\downarrow} + \text{H.c.}), \end{aligned} \tag{2}$$

where U and U' are intra-orbital, inter-orbital Coulomb interactions, respectively, and J represents the exchange and pair-hooping interactions. Throughout the paper, the condition $U = U' + 2J$ is assumed.

The energy band structure and the FSs obtained from H_0 [Eq. (1)] are shown in Fig. 1. The α band forms a hole-like FS centered at (π, π) while the β band forms an electron-like FS centered at $(0, 0)$. Both bands have flat and nested FSs and thus the Peierls fluctuations due to the presence of one-dimensional FSs can be expected.

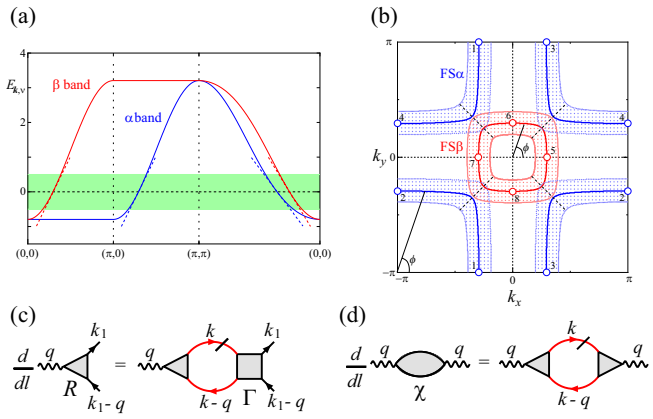

FIG. 1: (Color online) (a) Band structure of H_0 for $n = 1.2$. The linearized band dispersions are shown by the dashed lines. The low-energy excitations of electrons ($|\xi^{\rm linear}_{\boldsymbol{k},\nu}| \leq \Lambda_0$) are denoted by the shaded area. (b) The patch index ($1 \sim 8$) on the FSs. (c, d) The diagrammatic representation of the scaling equations for the three-point vertex R and the susceptibility χ, where l is the scaling parameter. The slashed line represents an electron propagation having the energy on the shell $\Lambda_{l+dl} < |\xi^{\rm linear}_{\boldsymbol{k},\nu}| < \Lambda_l$.

We apply the RG method to this two-band system. The scattering processes of electrons having energies less than the bandwidth cutoff Λ_0 are integrated within the one-loop RG scheme [24]. The low-energy parts of band structure are denoted by the shaded area in Fig. 1 (a). In order to analyze low-temperature properties accurately, we linearize the band dispersion within the cutoff scale Λ_0 and change the $\boldsymbol{k}$ summation into the energy (ξ) integration [25]. In the bandwidth-cutoff RG scheme, the ξ integration is replaced by the energy-shell integration $\Lambda_{l+dl} < |\xi| < \Lambda_l$, where $\Lambda_l = \Lambda_0 e^{-l}$ and l is the logarithmic scaling parameter. We can analyze low-temperature (T) behavior by integrating the RG equations up to the scale $l \sim \ln(\Lambda_0/T)$, unless the one-loop RG breaks down due to the divergence of coupling constants. The linearized dispersions, which are shown by the dotted lines in Fig. 1 (a), are given by $\xi^{\rm linear}_{\boldsymbol{k},\nu} = v^x_{F\nu}(\phi)\,[k_x - k^x_{F\nu}(\phi)] + v^y_{F\nu}(\phi)\,[k_y - k^y_{F\nu}(\phi)]$ where $\nu = \alpha, \beta$ represents the band index. Here, we have introduced the azimuthal angle ϕ (see Fig. 1) and the "radius" of the FS $k_{F\nu}(\phi)$ [25]. The neglected higher energy contributions ($> \Lambda_0$) would be less important for qualitative results, although this simplification might lead to slight underestimation of orbital and spin susceptibilities.

In the next step, we discretize the FSs into patches and introduce the patch-index dependence of vertex functions. Since the present system has flat FSs, we expect that $\boldsymbol{k}$ dependence of vertex functions along the flat FSs would be small. In the present analysis we introduce four patches per each band: the total number of patches is $N_p = 8$. The patch label is shown in Fig. 1 (b). The FSs on the even (odd) number of patches are composed of the d_{xz} (d_{yz}) orbital completely. In convention, we ignored the Matsubara-frequency dependence of the vertex function, and the Matsubara frequencies of the external field operators are set to $i\omega_m \to 0$. The external momenta of vertices are also projected onto the points shown in Fig. 1 (b).

In order to analyze the dominant fluctuations in the present two-orbital system, we calculate the susceptibilities by using the RG method. Since this system has flat FSs, the spin susceptibility $\chi^{\rm s}(\boldsymbol{q})$ is expected to be enhanced at the nesting vector $\boldsymbol{q} = \boldsymbol{Q}$. The main purpose of the present paper is to analyze the quadrupole (orbital) susceptibility at low temperatures. In the present model, there are two irreducible quadrupole operators [26, 27]:

$$\hat{O}^j_{x^2-y^2} = \sum_\sigma (c^\dagger_{j,1,\sigma} c_{j,1,\sigma} - c^\dagger_{j,2,\sigma} c_{j,2,\sigma}) = n_{j,1} - n_{j,2}, \quad (3)$$

$$\hat{O}^j_{xy} = \sum_\sigma (c^\dagger_{j,1,\sigma} c_{j,2,\sigma} + c^\dagger_{j,2,\sigma} c_{j,1,\sigma}), \quad (4)$$

where j is the site index. The quadrupole susceptibility per spin is given by ($\gamma = x^2 - y^2$ and xy)

$$\chi^{\rm q}_\gamma(\boldsymbol{q}) = \frac{1}{2}\int_0^\beta d\tau \left\langle T_\tau \hat{O}_\gamma(\boldsymbol{q},\tau)\, \hat{O}_\gamma(-\boldsymbol{q},0)\right\rangle, \quad (5)$$

where τ is the imaginary time and $\beta = 1/(k_B T)$. Hereafter we consider only the case $\gamma = x^2 - y^2$ and denote $\chi^{\rm q}(\boldsymbol{q}) \equiv \chi^{\rm q}_{x^2-y^2}(\boldsymbol{q})$, since $\chi^{\rm q}_{xy}(\boldsymbol{q})$ is very small. The divergence of $\chi^{\rm q}(\boldsymbol{q} = \boldsymbol{0})$ reflects the emergence of the orbital nematic state ($\langle n_{xz}\rangle \neq \langle n_{yz}\rangle$), which is consistent with the nematic phase in $Sr_3Ru_2O_7$. In addition, we analyze the charge susceptibility $\chi^{\rm c}(\boldsymbol{q}) = \frac{1}{2}\int_0^\beta d\tau \langle T_\tau n(\boldsymbol{q},\tau) n(-\boldsymbol{q},0)\rangle$ where $n(\boldsymbol{q},\tau)$ is the charge density operator.

The RG equations for the susceptibilities are shown in Figs. 1 (c) and (d), where R and Γ are the three- and four-point vertices, respectively [24, 25]. In the one-loop RG method, Γ is calculated by solving parquet equations [24]. For the initial values of the susceptibilities, we have used the constrained RPA (cRPA) results, $\chi^z|_{l=0} = \chi^z_{\rm cRPA}$ ($z = {\rm s}, {\rm q}, {\rm c}$) [25]. The cRPA is obtained by the "constraint" non-interacting susceptibility χ^{0c}, which is given by omitting the low-energy integration less than Λ_0. The temperature dependence of χ^z is mainly caused by the four-point vertex Γ since cRPA shows weak temperature dependence. In the present numerical study, we put the electron filling $n = 0.8$, where the best nesting vector is given by $\boldsymbol{Q} \approx (0.4\pi, 0.4\pi)$. We choose the bandwidth cutoff $\Lambda_0 = 0.25$.

In the RPA without VCs [19, 27], $\chi^{\rm s(q)}_{\rm RPA}(\boldsymbol{q})$ is mainly enhanced by U (U'), and both of them have peak structures at $\boldsymbol{q} = \boldsymbol{Q}$ due to the nesting of FSs. $\chi^{\rm s}_{\rm RPA}(\boldsymbol{Q})$ is always larger than $\chi^{\rm q}_{\rm RPA}(\boldsymbol{Q})$ for the realistic parameter $U > U'$. We stress that $\chi^{\rm q}_{\rm RPA}(\boldsymbol{q} = \boldsymbol{0})$ exhibits no singularity, meaning that the nematic order is not realized in the RPA. In the following, we will show that $\chi^{\rm q}(\boldsymbol{q} = \boldsymbol{0})$ given by RG is strongly enhanced because of the VCs.

First, we focus on the case with $U = U'$. The T dependencies of the spin, quadrupole, and charge susceptibilities are shown in Fig. 2 (a). For comparison, the non-interacting results are also shown. Due to the interaction effects, both $\chi^{\rm s}(\boldsymbol{Q})$ and $\chi^{\rm q}(\boldsymbol{0})$ are enhanced, while $\chi^{\rm c}(\boldsymbol{0})$ is suppressed. The most striking feature is the critical enhancement of $\chi^{\rm q}(\boldsymbol{0})$

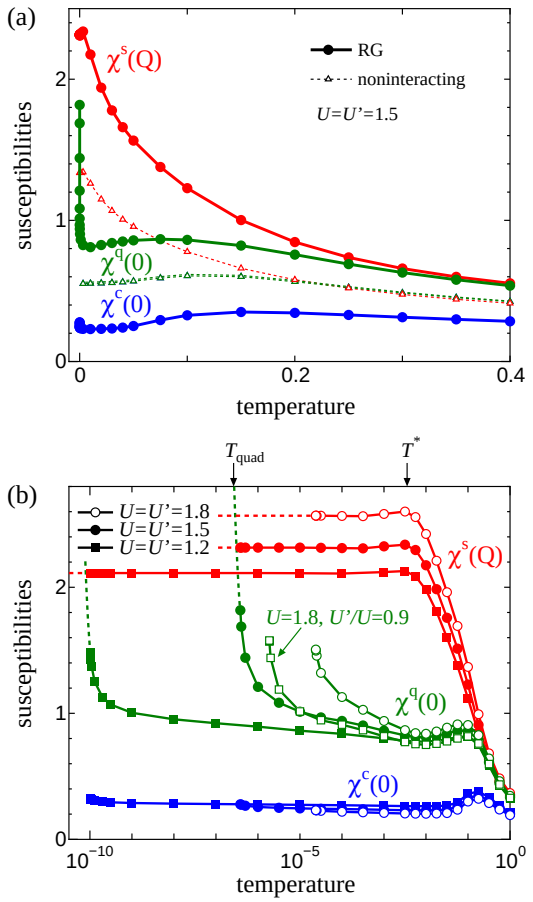

FIG. 2: (Color online) (a) Temperature dependencies of $\chi^{\rm s}(\boldsymbol{Q})$, $\chi^{\rm q}(\boldsymbol{0})$ and $\chi^{\rm c}(\boldsymbol{0})$ for $n = 0.8$. The solid lines represent the RG results, and the non-interacting results (dotted line) are also shown. (b) The susceptibilities obtained by the RG method in the logarithmic scale of T, for several choices of U and U' The dashed curves are the guides for eyes.

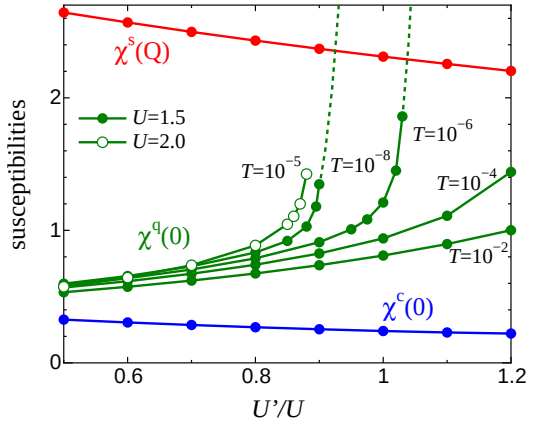

FIG. 3: (Color online) The U'/U dependencies of $\chi^{\rm q}(\boldsymbol{0})$ for several choice of temperatures. $\chi^{\rm s}(\boldsymbol{Q})$ and $\chi^{\rm c}(\boldsymbol{0})$ are also shown for $T = 10^{-4}$, which are almost temperature independent for $T < T^*$. The dashed curves are the guides for eyes.

at low temperatures, which cannot be obtained from RPA. We stress that the enhancement in $\chi^{\rm q}(\boldsymbol{q})$ is restricted to the $\boldsymbol{q} \approx \boldsymbol{0}$ region, indicating the emergence of the orbital nematic order.

The T dependencies of the susceptibilities given by the RG method are shown in Fig. 2 (b), for several choices of U. The spin susceptibility $\chi^{\rm s}(\boldsymbol{Q})$ is enhanced by the combined effect of the FS nesting and the on-site interaction U, from high temperatures. On the other hand, $\chi^{\rm s}(\boldsymbol{Q})$ is almost T independent below $T^* \sim 10^{-2}$ due to the effect of nesting deviation. Such a behavior is reminiscent of the Peierls instability in Q1D systems [28]. The quadrupole susceptibility $\chi^{\rm q}(\boldsymbol{0})$ starts to increase at $T \sim 10^{-2}$ and shows a divergent behavior at $T \approx T_{\rm quad}$. In the one-loop RG method, precise calculations of the $\boldsymbol{q} = \boldsymbol{0}$ mode in susceptibilities tend to be difficult at low temperatures, in case that the coupling Γ_l diverges before the convergence of the l integration in $\chi^z(\boldsymbol{0})$ is achieved [14, 29]. For this reason, we show the susceptibilities for $T > T_{\rm quad}$, where the one-loop RG method is qualitatively reliable. In contrast, $\chi^{\rm c}(\boldsymbol{0})$ shows no anomaly even at $T \sim T_{\rm quad}$, which would ensure the reliability of the singular behavior in $\chi^{\rm q}(\boldsymbol{0})$. For larger U, the critical enhancement of $\chi^{\rm q}(\boldsymbol{0})$ shits to high temperatures. For $U = 1.8$, $T_{\rm quad}$ is increased to $10^{-5} \sim 10^{-4}$, which corresponds to $\sim$ 1K if $t = 1$ eV.

We stress that the singular behavior in $\chi^{\rm q}(\boldsymbol{0})$ is also realized for $U'/U = 0.9$, as shown in Fig. 2 (b). Thus, high $T_{\rm quad}$ can be obtained even for $J > 0$ in the strongly-correlated cases. The U'/U dependencies of $\chi^{\rm q}(\boldsymbol{0})$ for $U = 1.5$ and 2.0 are shown in Fig. 3, with several choices of T. At $T \gtrsim 10^{-2}$, all susceptibilities exhibit linear dependencies in U', since the VCs are not important at higher temperatures. At low temperatures, in contrast, the strong enhancement of $\chi^{\rm q}(\boldsymbol{0})$ is seen for $U'/U \gtrsim 0.8$, which corresponds to $J/U \lesssim 0.1$.

Here, we discuss the reason why $\chi^{\rm q}(\boldsymbol{q})$ is critically enhanced only for $\boldsymbol{q} \approx \boldsymbol{0}$ in the RG analysis. The enhancement of the $\boldsymbol{q} \approx \boldsymbol{0}$ mode is a strong hallmark of the dominant contributions of the Aslamazov-Larkin (AL) type VCs, since these VCs are known as the enhancement mechanisms of $\boldsymbol{q} \approx \boldsymbol{0}$ susceptibilities. As shown in Refs. 23 and 27, the AL term due to the magnetic fluctuations [Fig. 4 (a)] gives the enhancement of $\chi^{\rm q}(\boldsymbol{0})$. In addition, we will show the importance of the *AL term due to the superconducting fluctuations* [Fig. 4 (b)], which is not discussed in Refs. 23 and 27. For this purpose, we introduce the effective interaction for ferro-orbital fluctuations $\Gamma^{\rm quad}$ and that for superconducting fluctuations $\Gamma^{{\rm SC}d}$, which give the quadrupole and d-wave superconducting susceptibilities:

$$\Gamma^{\rm quad} \equiv \frac{1}{N_p^2}\sum_{p,p'}[2\Gamma(p,p';p,p') - \Gamma(p,p';p',p)]\mathcal{O}_p\mathcal{O}_{p'}, \quad (6)$$

$$\Gamma^{{\rm SC}d} \equiv \frac{1}{2N_p^2}\sum_{p,p'}\Gamma(p,\bar{p};p',\bar{p}')\mathcal{D}_p\mathcal{D}_{p'}, \quad (7)$$

where $\mathcal{O}_p$ is the form factor for $\gamma = x^2 - y^2$ quadrupole: $\mathcal{O}_p = +1(-1)$ for odd (even) number of the patch index p.

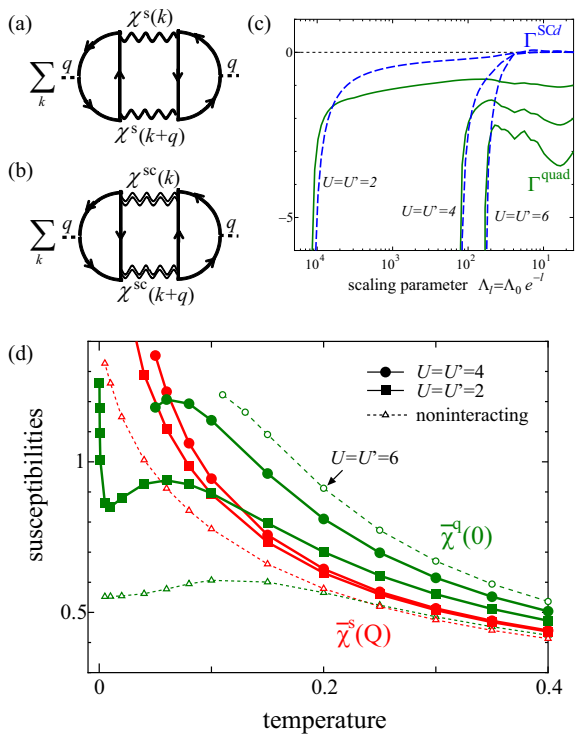

FIG. 4: (Color online) (a) The magnetic AL term and (b) the superconducting AL term, where $\chi^{\rm sc}(\boldsymbol{k})$ is superconducting propagator. They are proportional to $\sum_{\boldsymbol{k}} \chi^z(\boldsymbol{k})\,\chi^z(\boldsymbol{k}+\boldsymbol{q})$ $(z = {\rm s}, {\rm sc})$, which takes maximum value at $\boldsymbol{q} = \boldsymbol{0}$. (c) The scaling flows of the effective interactions $\Gamma^{\rm quad}$ and $\Gamma^{{\rm SC}d}$ at $T = 10^{-10}$. The large negative value of $\Gamma^{{\rm quad},{\rm SC}d}$ gives the enhancement of the corresponding susceptibility. (d) T dependence of $\bar{\chi}^{\rm q}(\boldsymbol{0})$ and $\bar{\chi}^{\rm s}(\boldsymbol{Q})$ for $U = U' \geq 2$. Here, we show results only in the temperature region where the one-loop RG method is qualitatively reliable.

Also, $\mathcal{D}_p$ is the d-wave form factor: $\mathcal{D}_p = +1(-1)$ for $p = 1, 3, 6, 8 (2, 4, 5, 7)$. The patch indices p and $\bar{p}$ are related by the inversion symmetry. The initial values are $\Gamma^{\rm quad}|_{l=0} = (3U - 5U')/2$ and $\Gamma^{{\rm SC}d}|_{l=0} = 0$.

The scaling flows of $\Gamma^{\rm quad}$ and $\Gamma^{{\rm SC}d}$ are shown in Fig. 4 (c) [30]. The obtained $\Gamma^{\rm quad}$ weakly depends on l at high energies, while it exhibits a steep increase in magnitude when $\Lambda_l \approx T_{\rm quad}$. This behavior gives the divergent behavior in $\chi^{\rm q}(\boldsymbol{0})$ observed in Fig. 2. Moreover, $\Gamma^{{\rm SC}d}$ also shows a steep increase in magnitude at $\Lambda_l \approx T_{\rm quad}$: This fact means that the development of $\chi^{\rm q}(\boldsymbol{0})$ is closely related to the superconducting fluctuations. From the diagrammatic arguments, we conclude that the major contribution is given by the superconducting AL term in Fig. 4 (b), which represents the coupling between the quadruple and superconducting fluctuations. This *superconducting-fluctuation-driven orbital nematic order* had not been pointed out previously. In two-dimensional systems, the orbital nematic order will occur above the superconducting transition, since the Ising-type quadrupole order is more robust than the XY-type superconducting order against thermal and quantum fluctuations.

Up to now, we focused on the weak interaction cases, in which the RG method works very well till very low temperatures. Now, we study the orbital fluctuations for larger Coulomb interactions. In Fig. 4 (d), the T dependencies of the quadrupole and spin susceptibilities are shown for $U = U' \geq 2$. Here, $\bar{\chi}^{\rm q,s}$ is obtained by solving Fig. 1 (d) with using the initial values $\bar{\chi}^{\rm q,s}_{l=0} = \chi^{0c}$. In this method, although the obtained values are underestimated, we can focus on the T dependence originating from the correlation effects within Λ_0. In Fig. 4 (d), $\bar{\chi}^{\rm q}(\boldsymbol{0})$ is enhanced by U even at higher temperatures, which cannot be attributed to the superconducting fluctuations. This enhancement originates from large $\Gamma^{\rm quad}$ in higher energy region $\Lambda_l \gtrsim 0.05$ in Fig. 4 (c). Both $\bar{\chi}^{\rm q}(\boldsymbol{0})$ and $\bar{\chi}^{\rm s}(\boldsymbol{Q})$ show similar Curie-Weiss behaviors, indicating that the enhancement of $\bar{\chi}^{\rm q}(\boldsymbol{0})$ originates from the spin fluctuations. Therefore, the magnetic AL term in Fig. 4 (a) is the natural origin of the enhancement of $\bar{\chi}^{\rm q}(\boldsymbol{0})$ at higher temperatures. As the origin of the field-induced magnetic quantum criticality, both the van-Hove singularity [9–12] and the field-suppression of quantum fluctuation [31] mechanisms had been discussed previously.

In summary, the orbital Pomeranchuk instability driven by superconducting and magnetic quantum criticalities had been confirmed by the RG method. In the weak-interaction case ($U \lesssim 2$), where the RG method is trusted well, $\chi^{\rm q}(\boldsymbol{0})$ is critically enhanced by the AL-type VC due to the superconducting fluctuations. In addition, we studied the strong-interaction case, and also found the development of $\chi^{\rm q}(\boldsymbol{0})$ driven by the spin fluctuations, consistently with the perturbation analysis in Ref. 27. Both mechanisms would contribute to the nematic phase in $Sr_3Ru_2O_7$, although magnetic AL term might be more important under the strong magnetic field. The present mechanisms of orbital nematic phase would be realized in various multiorbital systems.

The authors thank fruitful discussions with Mr. Y. Ohno and Prof. D.S. Hirashima. This work was supported by Grant-in-Aid for Scientific Research from the Ministry of Education, Culture, Sports, Science, and Technology, Japan.

[1] S. A. Grigera, R. S. Perry, A. J. Schofield, M. Chiao, S. R. Julian, G. G. Lonzarich, S. I. Ikeda, Y. Maeno, A. J. Millis, and A. P. Mackenzie, Science **294**, 329 (2001).
[2] R. Perry, L. Galvin, S. Grigera, L. Capogna, A. Schofield, A. Mackenzie, M. Chiao, S. Julian, S. Ikeda, S. Nakatsuji, et al., Phys. Rev. Lett. **86**, 2661 (2001).
[3] S. Grigera, R. Borzi, A. Mackenzie, S. Julian, R. Perry, and Y. Maeno, Phys. Rev. B **67**, 214427 (2003).
[4] A. P. Mackenzie, J. A. N. Bruin, R. A. Borzi, A. W. Rost, and S. A. Grigera, Physica C **481**, 207 (2012), and references therein.
[5] K. Kitagawa, K. Ishida, R. Perry, T. Tayama, T. Sakakibara, and Y. Maeno, Phys. Rev. Lett. **95** (2005).
[6] S. A. Grigera, P. Gegenwart, R. A. Borzi, F. Weickert, A. J. Schofield, R. S. Perry, T. Tayama, T. Sakakibara, Y. Maeno, A. G. Green, et al., Science **306**, 1154 (2004).
[7] R. A. Borzi, S. A. Grigera, J. Farrell, R. S. Perry, S. J. S. Lis-

ter, S. L. Lee, D. A. Tennant, Y. Maeno, and A. P. Mackenzie, Science **315**, 214 (2007).
[8] C. J. Halboth and W. Metzner, Phys. Rev. Lett. **85**, 5162 (2000).
[9] H. Yamase and A. A. Katanin, J. Phys. Soc. Jpn. **76**, 073706 (2007).
[10] H. Yamase, Phys. Rev. B **80**, 115102 (2009).
[11] M. H. Fischer and M. Sigrist, Phys. Rev. B **81**, 064435 (2010).
[12] H. Yamase and P. Jakubczyk, Phys. Rev. B **82**, 155119 (2010).
[13] Y. Yoshioka and K. Miyake, J. Phys. Soc. Jpn. **81**, 023707 (2012).
[14] C. Honerkamp and M. Salmhofer, Phys. Rev. B **64**, 184516 (2001).
[15] C. Honerkamp, Phys. Rev. B **72**, 115103 (2005).
[16] S. Raghu, A. Paramekanti, E. Kim, R. Borzi, S. Grigera, A. Mackenzie, and S. A. Kivelson, Phys. Rev. B **79**, 214402 (2009).
[17] W.-C. Lee and C. Wu, Phys. Rev. B **80**, 104438 (2009).
[18] K. W. Lo, W.-C. Lee, and P. W. Phillips, arXiv:1207.4206.
[19] T. Takimoto, Phys. Rev. B **62**, 14641 (2000).
[20] J.-H. Chu, J. G. Analytis, K. De Greve, P. L. McMahon, Z. Islam, Y. Yamamoto, and I. R. Fisher, Science **329**, 824 (2010).
[21] M. Yoshizawa, D. Kimura, T. Chiba, S. Simayi, Y. Nakanishi, K. Kihou, C.-H. Lee, A. Iyo, H. Eisaki, M. Nakajima, et al., J. Phys. Soc. Jpn. **81**, 024604 (2012), and references therein.
[22] R. Fernandes, L. VanBebber, S. Bhattacharya, P. Chandra, V. Keppens, D. Mandrus, M. McGuire, B. Sales, A. Sefat, and J. Schmalian, Phys. Rev. Lett. **105**, 157003 (2010).
[23] S. Onari and H. Kontani, arXiv:1203.2874.
[24] C. Halboth and W. Metzner, Phys. Rev. B **61**, 7364 (2000).
[25] T. Nishine, M. Tsuchiizu, and Y. Suzumura, J. Phys.: Conf. Ser. **132**, 012020 (2008).
[26] H. Kontani, T. Saito, and S. Onari, Phys. Rev. B **84** (2011).
[27] Y. Ohno, M. Tsuchiizu, S. Onari, and H. Kontani, arXiv (2012).
[28] R. Duprat and C. Bourbonnais, Eur. Phys. J. B **21**, 219 (2001).
[29] H. Nelisse, C. Bourbonnais, H. Touchette, Y. M. Vilk, and A. M. Tremblay, Eur. Phys. J. B **12**, 351 (1999).
[30] We have verified that the similar scaling behavior of $\Gamma^{\rm quad}$ to Fig. 4 (c) is obtained by the T-flow RG scheme [14].
[31] K. Sakurazawa, H. Kontani, and T. Saso, J. Phys. Soc. Jpn. **74**, 271 (2005).